

AD-A219 135

DTIC FILE COPY

AD

4

TECHNICAL REPORT ARCCB-TR-90003

**FRACTURE MECHANICS ASSESSMENT OF
A CRACKED 16-INCH INNER DIAMETER
1945 VINTAGE-JACKETED PRESSURE VESSEL**

J. A. KAPP

R. R. FUJCAK

M. D. WITHERELL

T. M. HICKEY

J. J. ZALINKA

JANUARY 1990

DTIC
ELECTE
MAR 2 1990
S B D



**US ARMY ARMAMENT RESEARCH,
DEVELOPMENT AND ENGINEERING CENTER
CLOSE COMBAT ARMAMENTS CENTER
BENÉT LABORATORIES
WATERVLIET, N.Y. 12189-4050**



APPROVED FOR PUBLIC RELEASE; DISTRIBUTION UNLIMITED

90 03 01 143

DISCLAIMER

The findings in this report are not to be construed as an official Department of the Army position unless so designated by other authorized documents.

The use of trade name(s) and/or manufacturer(s) does not constitute an official indorsement or approval.

DESTRUCTION NOTICE

For classified documents, follow the procedures in DoD 5200.22-M, Industrial Security Manual, Section II-19 or DoD 5200.1-R, Information Security Program Regulation, Chapter IX.

For unclassified, limited documents, destroy by any method that will prevent disclosure of contents or reconstruction of the document.

For unclassified, unlimited documents, destroy when the report is no longer needed. Do not return it to the originator.

REPORT DOCUMENTATION PAGE		READ INSTRUCTIONS BEFORE COMPLETING FORM
1. REPORT NUMBER ARCCB-TR-90003	2. GOVT ACCESSION NO.	3. RECIPIENT'S CATALOG NUMBER
4. TITLE (and Subtitle) FRACTURE MECHANICS ASSESSMENT OF A CRACKED 16-INCH INNER DIAMETER 1945 VINTAGE-JACKETED PRESSURE VESSEL		5. TYPE OF REPORT & PERIOD COVERED Final
		6. PERFORMING ORG. REPORT NUMBER
7. AUTHOR(s) J. A. Kapp, M. D. Witherell, R. R. Fajczak, T. M. Hickey, and J. J. Zalinka		8. CONTRACT OR GRANT NUMBER(s)
9. PERFORMING ORGANIZATION NAME AND ADDRESS U.S. Army ARDEC Benet Laboratories, SMCAR-CCB-TL Watervliet, NY 12189-4050		10. PROGRAM ELEMENT, PROJECT, TASK AREA & WORK UNIT NUMBERS AMCMS No. 6111.02.H610.011 PRON No. 1A82Z8CANMSC
11. CONTROLLING OFFICE NAME AND ADDRESS U.S. Army ARDEC Close Combat Armaments Center Picatinny Arsenal, NJ 07806-5000		12. REPORT DATE January 1990
		13. NUMBER OF PAGES 19
14. MONITORING AGENCY NAME & ADDRESS (if different from Controlling Office)		15. SECURITY CLASS. (of this report) UNCLASSIFIED
		15a. DECLASSIFICATION/DOWNGRADING SCHEDULE
16. DISTRIBUTION STATEMENT (of this Report) Approved for public release; distribution unlimited.		
17. DISTRIBUTION STATEMENT (of the abstract entered in Block 20, if different from Report)		
18. SUPPLEMENTARY NOTES Presented at the 1988 ASME Pressure Vessel and Piping Conference, Pittsburgh, PA, June 1988. Published in Proceedings of the Conference.		
19. KEY WORDS (Continue on reverse side if necessary and identify by block number) Pressure Vessels Fracture Mechanics Fatigue Life Predictions		
20. ABSTRACT (Continue on reverse side if necessary and identify by block number) A fracture mechanics assessment of the structural integrity of a very large 1945 vintage pressure vessel has been performed. Many of these old vessels had not been used for several years and have only recently been returned to service. After a relatively short number of pressure cycles, long, but shallow, longitudinal cracks were found in the vessels. The fracture assess- ment included the development of a stress intensity factor solution for the vessel using finite elements, and the measurement of both the fracture (CONT'D ON REVERSE)		

20. ABSTRACT

toughness and fatigue crack propagation rates for the two steels from which the liner of the vessel was made. A wide range expression was fit to the numerically determined stress intensity factor solution and was used to determine the remaining life of the vessel. Failure of the vessel was assumed to be through fracture of the liner. The results indicate that this vessel has a significant remaining fatigue life.

UNCLASSIFIED

TABLE OF CONTENTS

	<u>Page</u>
INTRODUCTION	1
PROCEDURE	1
RESULTS	3
Material Property Measurements	3
Stress Analysis Results	5
FATIGUE CRACK GROWTH PREDICTIONS	7
CONCLUSION	9
REFERENCES	10

TABLES

I. FRACTURE PROPERTIES OF LINER MATERIALS	3
---	---

LIST OF ILLUSTRATIONS

1. Schematic of a 16-inch pressure vessel	11
2. Crack growth rate versus ΔK	12
3. Crack growth rate versus K_{max}	13
4. Normalized K solution for internal pressure loading	14
5. Normalized K solution for shrink fit loading	15
6. Specific K solution for 43 Ksi internal pressure	16
7. Specific K solution for 49.7 Ksi internal pressure	17
8. Remaining life predictions	18

Accession For	
NTIS GRA&I	<input checked="" type="checkbox"/>
DTIC TAB	<input type="checkbox"/>
Unannounced	<input type="checkbox"/>
Justification	
By _____	
Distribution/	
Availability Codes	
Dist	Avail and/or Special
A-1	

INTRODUCTION

Many very large 16-inch inner diameter (ID)-jacketed thick-walled pressure vessels manufactured about 1945 have recently been returned to service. These vessels are of a jacketed design as shown schematically in Figure 1. Long, but shallow, longitudinal ID cracks have appeared in some of these vessels during repeated pressurization. The purpose of this report is to establish the tolerance of the vessels to the presence of these cracks.

PROCEDURE

To establish the damage tolerance of any structure, first the material's fracture properties must be determined. Second, the stress intensity factors that are applied to the structure during load application must be calculated. And finally, using both of these results the critical flaw size and the number of loadings that will grow the crack to that size can be predicted.

The fracture mechanics properties required are the fracture toughness of the material (K_{IC}) and the fatigue crack growth rate as a function of the applied stress intensity factor (dl/dN versus ΔK). The fracture toughness properties were measured from the largest samples that could be machined from the liner material (the liner is the innermost segment of the vessel and is the structural component that cracked). The specimen design was the compact tension-type sample with a through-thickness dimension of 1.5 inches [C(T)-1.5T]. The crack propagation data were also obtained from the liner material. The specimen design for this was a pure bending sample. This specimen could be loaded so that negative loading ratios could be applied which would simulate the effects of compressive residual stress due to the interference fit between the liner and the outer jackets of the vessel. Crack growth rate data

were obtained at two loading ratios, one where the loads went from zero to tension loading and the other for fully-reversed loading.

As previously stated, in order to predict critical flaw sizes and determine remaining life, the stress intensity factor solution for the structure under load must be determined. For simple cases, this can either be estimated or found in the literature. The K solution for this specific geometry was developed using finite element analysis, since there were no solutions in the literature for the specific geometry of the 16-inch vessel.

The finite element routine used was the ABAQUS (ref 1) general purpose program. This code was developed to analyze nonlinear problems, but it also has an excellent linear analysis capability. In addition, the specialized features necessary to determine stress intensity factors have also been incorporated into the code.

Since the actual 16-inch vessel was of a jacketed design, special modeling methods were needed. Under elastic conditions, the total stresses in the liner of the vessel were calculated as the superposition of the residual compression due to the shrink fit plus the tension produced by the internal pressure. This was modeled by solving two separate problems. First, the shrink fit was produced by modeling the liner and the external jackets as separate structures, tying them together using multiple-point constraints, and then applying a thermal load that expanded the liner into the jackets. This produced the shrink fit compression in the liner in exactly the same manner as the physical loading on the liner. For the internal pressure case, the vessel was modeled as above

¹"ABAQUS User's Manual," Version 4.5(a), Hibbitt, Karlsson, and Sorensen, Inc., Providence, RI, July 1985.

(liner and jacket separate, then tied together) and internal pressure was applied at the ID and along the crack faces.

RESULTS

Material Property Measurements

The fracture toughness measurements are presented in Table I. As is readily apparent, the two liners have substantially different properties. The reasons are explained by the metallurgical examination of these liners conducted by Tauscher (ref 2). One liner had a predominantly ferrite/bainite

TABLE I. FRACTURE PROPERTIES OF LINER MATERIALS

Specimen Identification	Test Temperature (°C)	Fracture Toughness (Ksi√in.)	Micostructure	Valid (Y/N)
A-4	25	>> 90.4	F/B	N
A-2	25	>>106.7	F/B	N
B-1	25	90.4	P	Mar
B-4	25	82.0	P	Mar
B-2	-40	63.1	P	Y
B-3	-40	58.9	P	Y
A-1	-40	108.9	F/B	N
A-3	-40	89.7	F/B	Mar

Key:

P: Pearlitic Microstructure

F/B: Ferrite/Bainite Microstructure

Mar: Marginally Valid

1 Ksi√in. = 1.099 MPa√m

²S. Tauscher, "Metallurgical Assessment of Two Liner Materials," Memorandum For the Record, Engineering Support Division, Benet Laboratories, U.S. Army ARDEC, Watervliet, NY, July 1987.

microstructure (Liner A), while the second had a predominantly pearlitic microstructure (Liner B). The vast difference in fracture properties was expected since it was well known that the fracture properties of the class of steels examined with pearlitic microstructures were very inferior to the fracture properties of the same steel at the same strength with a ferrite/bainite microstructure. The fracture toughness properties presented in the table are the values obtained using the standard methods of analysis found in Reference 3. These numbers were invalid for the more ductile material and only marginally valid for the more brittle case. The actual properties were probably somewhat higher for the pearlitic liner and much higher for the ferrite/bainite liner. The values in Table I were used to predict the critical defect sizes for the vessels, since the use of these values yields a conservative prediction.

Although the fracture properties were quite different, the fatigue crack propagation properties of the two liners were not. The results, presented in graphical form in Figures 2 and 3, attempted to account for mean stress effects or R ratio effects. This was necessary if the effects of the residual stresses from the shrink fit were to be included in predicting the remaining fatigue life of cracked liners.

Figure 2 presents the crack growth data in the classical way. The crack growth rate (dl/dN) is plotted against the applied stress intensity factor range (ΔK). The straight line on the log-log plot suggests that the material property followed a power-law relationship and that there was a substantial effect due to the R ratio. Furthermore, it seems that there was no effect on fatigue crack propagation due to the different microstructures. The R ratio effect was

³"Standard Test Method for Plane-Strain Fracture Toughness of Metallic Materials, ASTM E-399," Annual Book of ASTM Standards, Vol. 03.01, American Society, for Testing and Materials, Philadelphia, PA, 1986.

expected because when R is -1 , substantial compressive loading is applied and this tends to retard fatigue crack propagation. In order to account for the crack growth retardation, the data are plotted differently in Figure 3. In this case, the crack growth rate is plotted against the maximum stress intensity factor applied during the fatigue cycle (K_{max}). It is readily observed that this formulation accounts for the R ratio effect that was measured. All of the data fell in a small scatter band. For crack propagation predictions, an upper limit power-law that represents the data in Figure 3 is also plotted in the figure. The equation for this power-law is

$$dl/dN = 9.8 \times 10^{-10} K_{max}^{2.86} \quad (1)$$

The unit of crack growth rate is inch/cycle and the unit of K_{max} is $Ksi\sqrt{in}$. When the units of crack growth rate are m/cycle and the units of K_{max} are $MPa\sqrt{m}$, Eq. (1) becomes

$$dl/dN = 1.9 \times 10^{-11} K_{max}^{2.86} \quad (1a)$$

Stress Analysis Results

The K solutions developed from the finite element analysis are plotted in Figure 4 for the internal pressure case and in Figure 5 for the shrink fit loading case. In both plots, the normalized stress intensity factors are given as a function of normalized crack depth. The value l is the physical crack depth, and W is the liner wall thickness ($b-a$). The stress intensity factor normalization is $K/\sigma_\theta(ID)\sqrt{\pi l}$, where K is the stress intensity factor and $\sigma_\theta(ID)$ is the tangential stress at the ID for the particular loading condition. For the case of internal pressure loading, $\sigma_\theta(ID)$ is the Lamé tangential stress at the ID plus the pressure that acts on the crack faces (ref 4)

⁴T. E. Davidson and D. P. Kendall, "The Design of Pressure Vessels for Very High Pressure Operation," The Mechanical Behavior of Materials Under Pressure, (H.L.D. Pugh, ed.), Elsevier Publishing Company, Amsterdam, 1970.

$$\sigma_{\theta}(ID) = \frac{2pk^2}{k^2-1} \quad (2)$$

In Eq. (2), p is the internal pressure and k is the overall radius ratio of the compound cylinder (the liner plus all of the jackets), or $k = OD$ (outer diameter)/ ID .

For the shrink fit loading case, the value of $\sigma_{\theta}(ID)$ is determined from the following equation (ref 4):

$$\sigma_{\theta}(ID) = \frac{-2b^2}{b^2-a^2} \frac{E\delta}{b} \left[\frac{(c^2-b^2)(b^2-a^2)}{2b^2(c^2-a^2)} \right] \quad (3)$$

In Eq. (3), b is the interference fit radius, E is Young's modulus of the material (both liner and jacket), δ is the amount of radial interference, and c is the outside radius of the overall built-up cylinder ($OD/2$).

To facilitate the use of the K solutions for the fatigue life predictions, it was necessary to fit an algebraic expression to the numerical results. This was easily accomplished by the use of the normalized solutions. We assume that K follows an equation as

$$K = \sigma_{\theta}(ID)\sqrt{\pi l} f(1/W) \quad (4)$$

For internal pressure loading,

$$f(1/W) = 1.12 - 0.175 \ 1/W - 0.515 \ (1/W)^2 + 1.43 \ (1/W)^3 \quad (5)$$

For shrink fit loading,

$$f(1/W) = 1.12 - 0.217 \ 1/W - 0.268 \ (1/W)^2 + 0.943 \ (1/W)^3 \quad (6)$$

Equations (5) and (6) are plotted along with the K solutions they represent in Figures 4 and 5. As can be seen in the figures, the agreement between the equations and the numerical results was excellent.

⁴T. E. Davidson and D. P. Kendall, "The Design of Pressure Vessels for Very High Pressure Operation," The Mechanical Behavior of Materials Under Pressure, (H.L.D. Pugh, ed.), Elsevier Publishing Company, Amsterdam, 1970.

FATIGUE CRACK GROWTH PREDICTIONS

Using the measured fatigue and fracture properties along with the K solutions generated, the remaining life of a cracked 16-inch liner can be predicted. This is done by rearranging Eq. (1) to a form in which it can be integrated

$$\Delta N = \int_{l_i}^{l_f} dl / (9.8 \times 10^{-10} K_{\max}^{2.86}) \quad (8)$$

In Eq. (7), l_i is the initial crack depth, l_f is the final crack depth, and ΔN is the number of cycles required to propagate the crack from l_i to l_f . The integral in Eq. (7) cannot be integrated exactly, but can be easily evaluated numerically using Simpson's rule or some other technique. This was done for the specific loading of a cracked 16-inch liner.

There are several specific variables that must be fixed for the integration to be performed. First, an initial crack depth has to be established. We assumed from heat checking that a crack of about 0.020 inch existed after the vessel was cycled once. Second, the pressure has to be established. There were two pressure ranges that could be applied to these vessels: (1) an internal pressure of 49.7 Ksi (342.7 MPa), and (2) an internal pressure of 43 Ksi (296.5 MPa). Third, the amount of shrink fit that was in the cylinder has to be established. In the highest stressed region, the required amount of interference was dimensioned as 0.020 + 0.001 inch (0.51 + 0.03 mm); 0.020 inch was used as the worst case.

The specific K solution for the lower pressure case (43 Ksi) is given in Figure 6 and that for the higher pressure case (49.7 Ksi) in Figure 7. These figures demonstrate how the total K solution was obtained. The stress intensity factor for internal pressure alone was determined for various crack depths. The stress intensity factor for the shrink fit loading was determined at the same

crack depths. The total K solution was found by point-by-point addition. As was expected, the 49.7 Ksi internal pressure case was worse than the 43 Ksi case. Using $80 \text{ Ksi}\sqrt{\text{in.}}$ ($88 \text{ MPa}\sqrt{\text{m}}$) as the fracture toughness of liners, the critical crack depth for a vessel subjected to 49.7 Ksi pressure was 0.25 inch (6.4 mm), while for the same vessel subjected to 43 Ksi pressure, the critical crack depth was about 0.38 inch (9.7 mm). If there were no shrink fit (a possible worst case), the critical crack depths for 49.7 Ksi pressure would be about 0.13 inch (3.3 mm) and for 43 Ksi pressure, about 0.20 inch (5.1 mm). These were the crack depths at which the integration of Eq. (7) was terminated.

The results of the integration (the predicted crack growth) are shown in Figure 8. In this plot, three cases are presented: 49.7 Ksi pressure and 43 Ksi pressure, both with a 0.020-inch interference, and 49.7 Ksi pressure with no interference. Again, these plots were generated assuming that the initial crack length was 0.020 inch. Assuming that fracture occurred at the critical crack depths determined above, the remaining lives for the three cases are as follows: for 49.7 Ksi with full interference fit, the remaining life was 3500 cycles; for 43 Ksi with full interference fit, the remaining life was 6700 cycles; and for 49.7 Ksi and no interference, the remaining life was about 1500 cycles.

The plots can also be used to determine the remaining life if the initial crack depth is more than 0.020 inch. For example, suppose that the measured existing crack is 0.050 inch (1 mm). We determine the remaining life for the 49.7 Ksi case as follows: the critical crack depth remains at 0.25 inch and the number of cycles to propagate a crack from 0.020 inch to 0.25 inch is 3500 cycles as from above. The number of cycles required to grow a crack from 0.020 inch to 0.050 inch for this case is about 1500 cycles. The 1500-cycle life has already been consumed leaving the difference as the remaining life for a crack

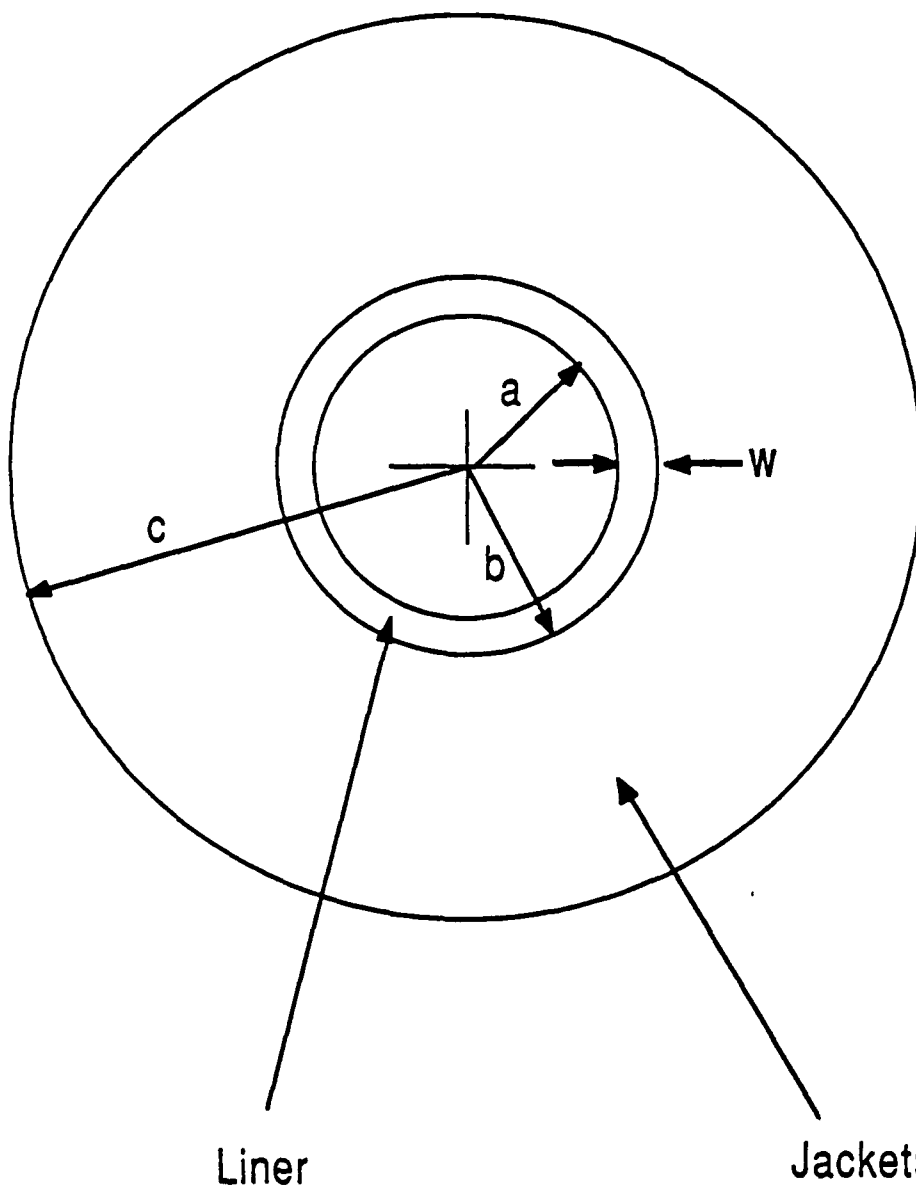
to grow from 0.050 inch to 0.25 inch or remaining life = $3500 - 1500 = 2000$ cycles. The same procedure can be followed for the other cases and any initial crack depth.

CONCLUSION

Fracture mechanics has been used to determine the resistance to the presence of cracks in 1945 vintage-jacketed thick-walled pressure vessels. The procedure required the measurement of fracture toughness and fatigue crack growth rates for two liner materials and the development of stress intensity factors for two loading conditions. The master crack growth rate curves developed can be used to assess the damage tolerance of these vessels, and to predict the remaining life with great accuracy.

REFERENCES

1. "ABAQUS User's Manual," Version 4.5(a), Hibbitt, Karlsson, and Sorensen, Inc., Providence, RI, July 1985.
2. S. Tauscher, "Metallurgical Assessment of Two Liner Materials," Memorandum For the Record, Engineering Support Division, Benet Laboratories, U.S. Army ARDEC, Watervliet, NY, July 1987.
3. "Standard Test Method for Plane-Strain Fracture Toughness of Metallic Materials, ASTM E-399," Annual Book of ASTM Standards, Vol. 03.01, American Society for Testing and Materials, Philadelphia, PA, 1986.
3. T. E. Davidson and D. P. Kendall, "The Design of Pressure Vessels for Very High Pressure Operation," The Mechanical Behavior of Materials Under Pressure, (H.L.D. Pugh, ed.), Elsevier Publishing Company, Amsterdam, 1970.



$a = 8.0$ in.
 $b = 10.16$ in.
 $c = 24.5$ in.

$$k = c/a = 3.06$$

Figure 1. Schematic of a 16-inch pressure vessel (1 in. = 2.54 cm).

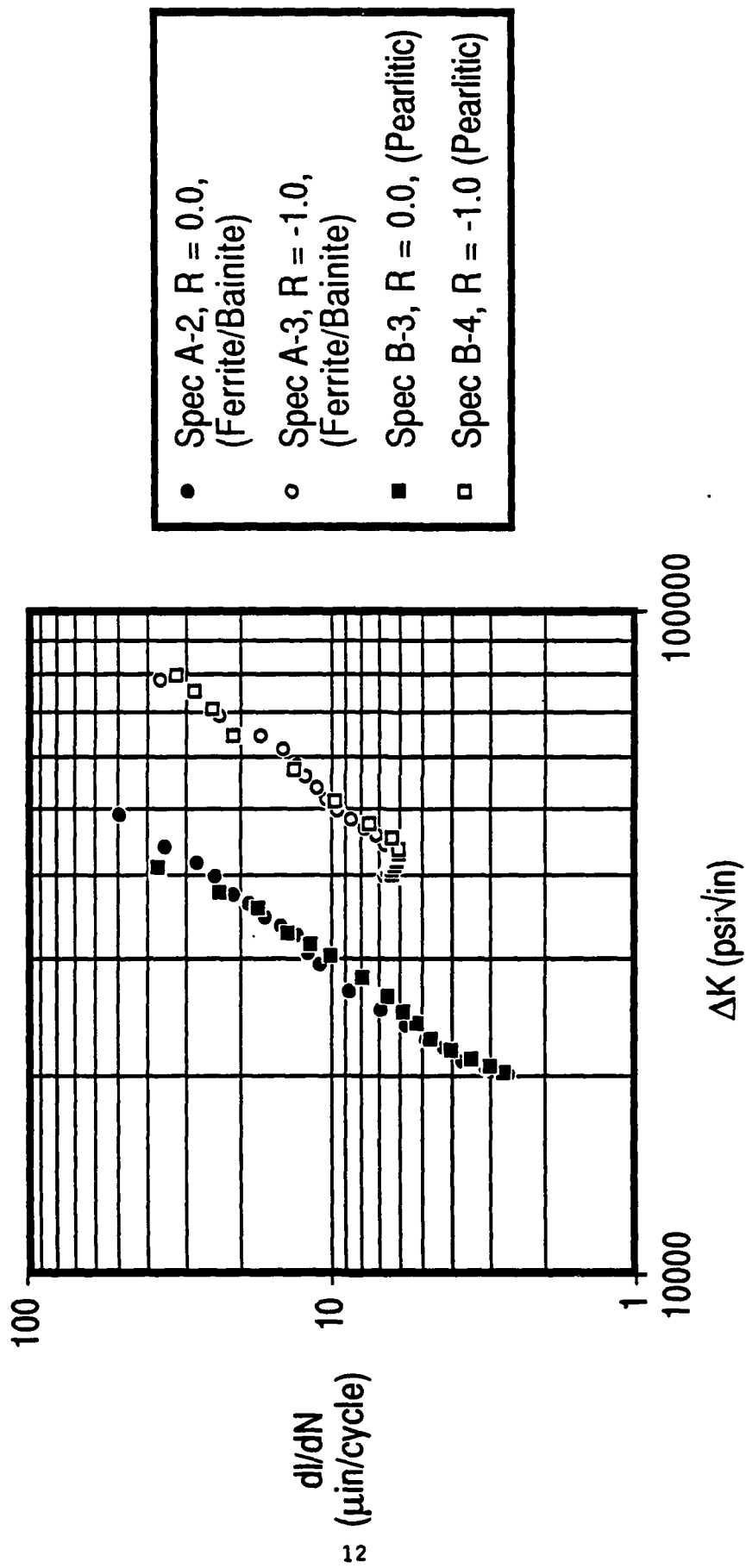


Figure 2. Crack growth rate versus ΔK (1 Ksi√in. = 1.099 MPa√m; 1 $\mu\text{in.}/\text{cycle}$ = 2.54×10^{-8} m/cycle).

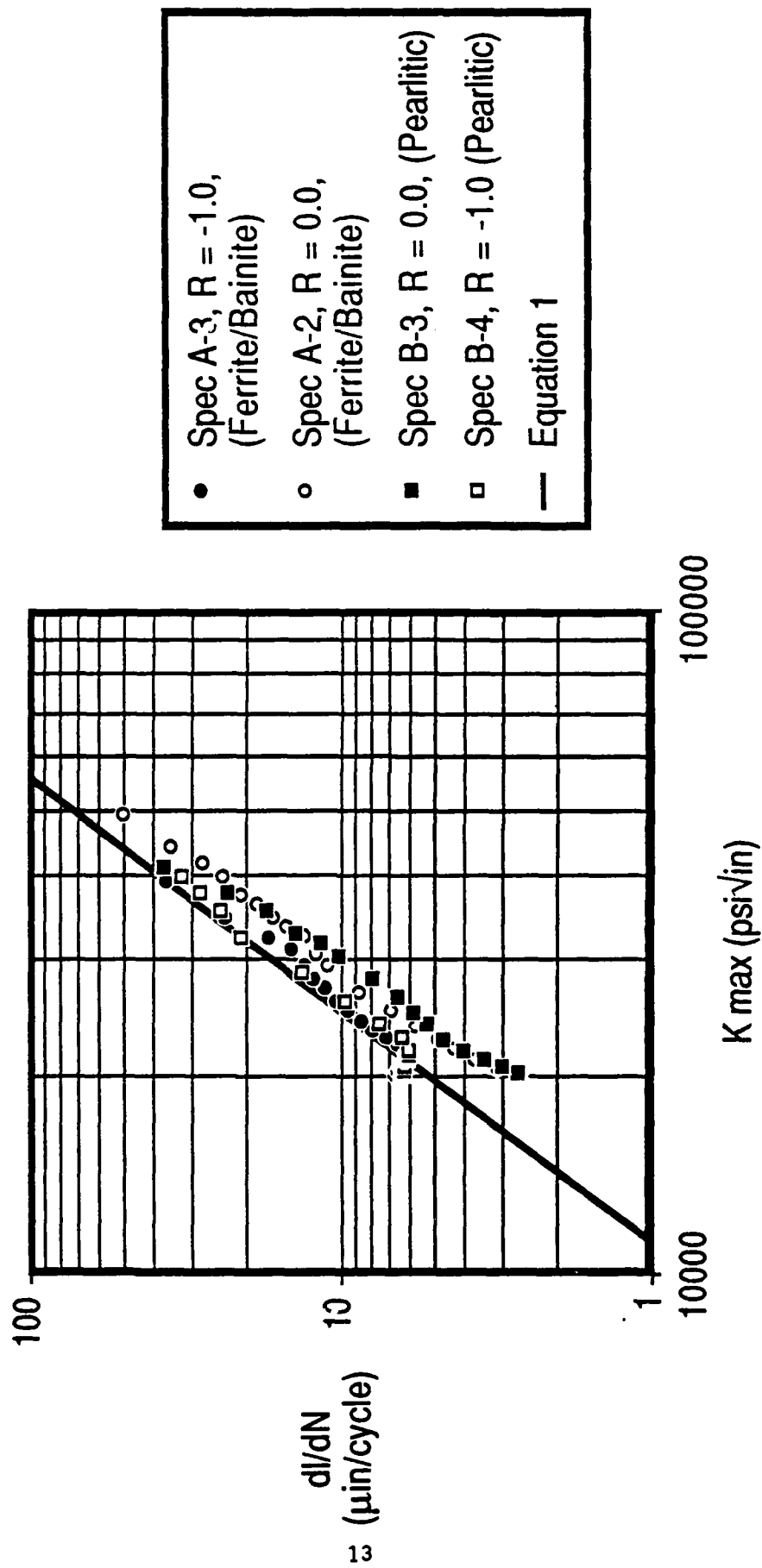


Figure 3. Crack growth rate versus K_{max} ($1 \text{ ksi}\sqrt{\text{in.}} = 1.099 \text{ MPa}\sqrt{\text{m}}$; $1 \text{ }\mu\text{in./cycle} = 2.54 \times 10^{-6} \text{ m/cycle}$).

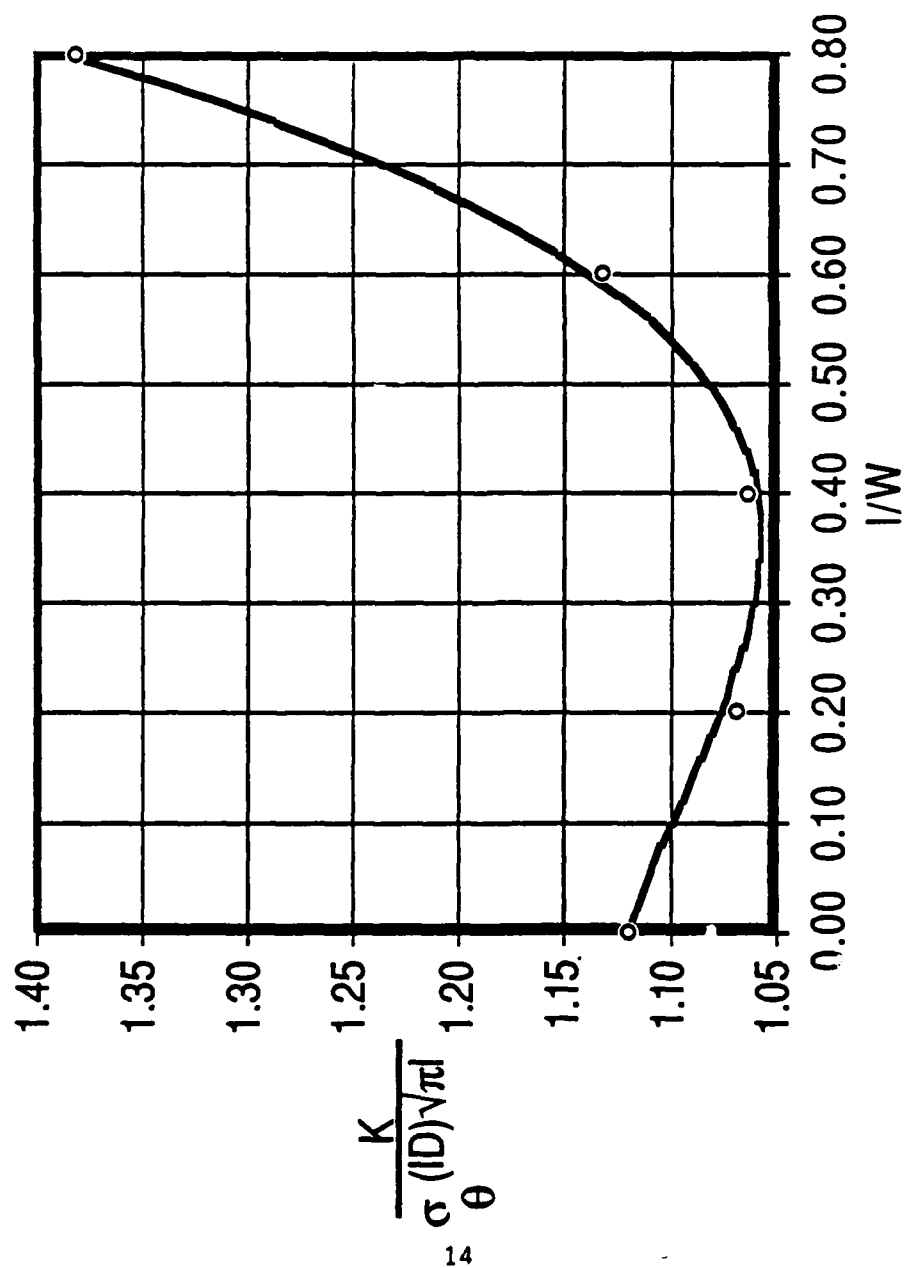
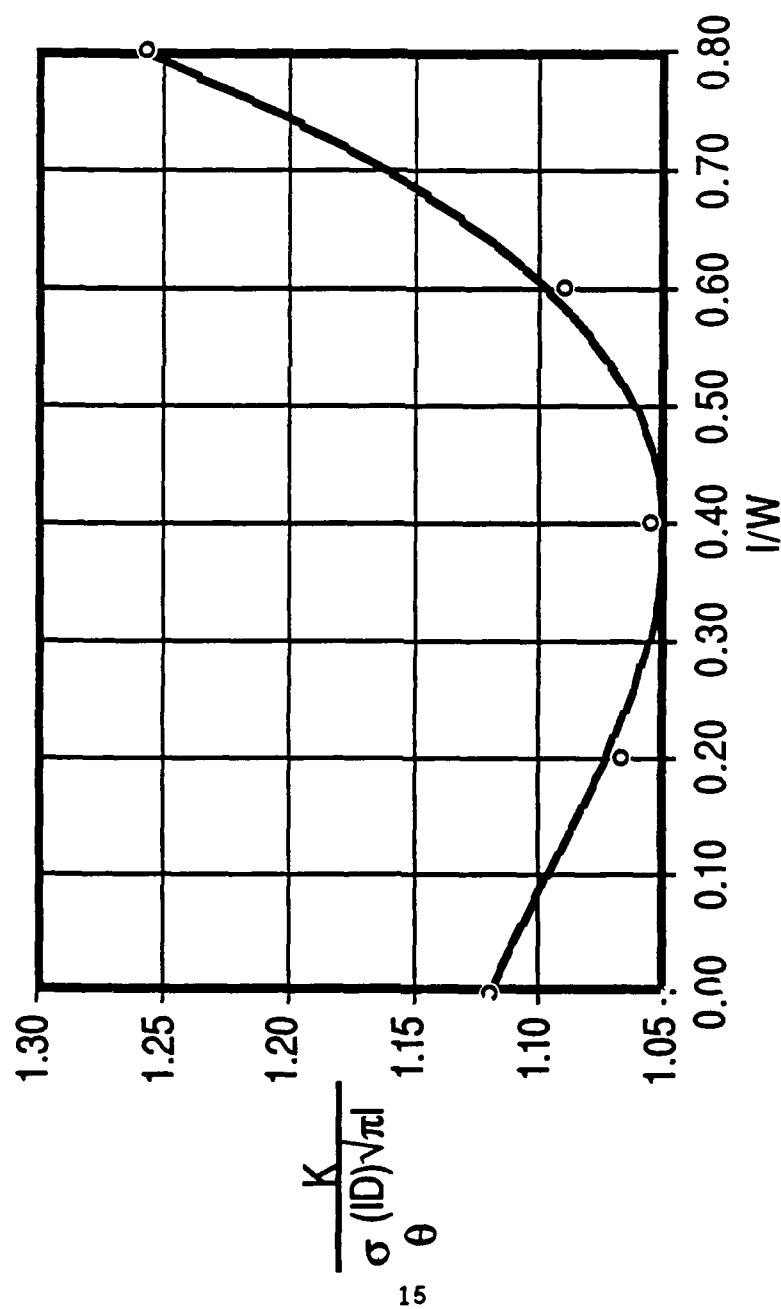


Figure 4. Normalized K solution for internal pressure loading.



— Equation 6
 ○ Finite Element Solution

Figure 5. Normalized K solution for shrink fit loading.

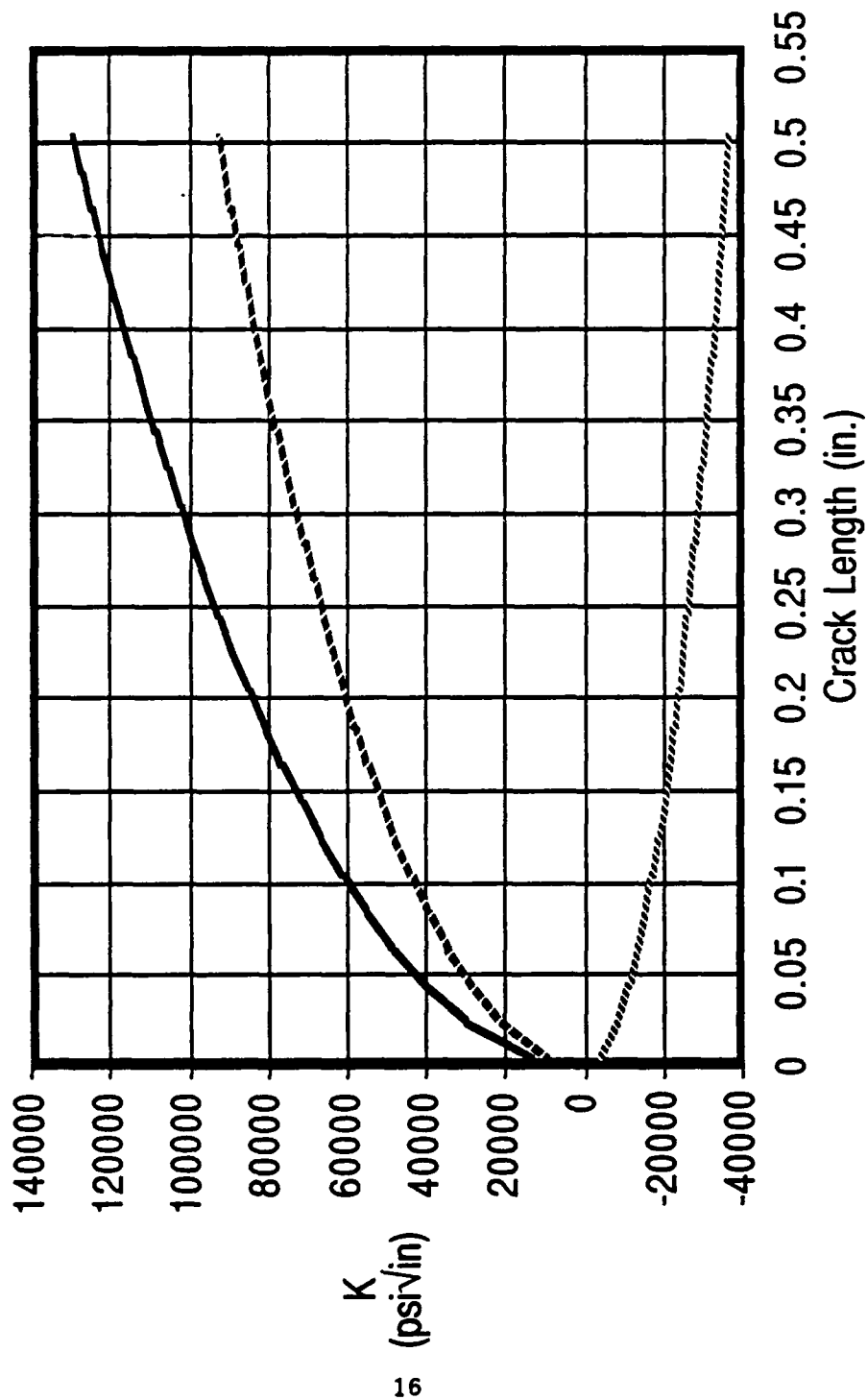


Figure 6. Specific K solution for 43 Ksi internal pressure (1 Ksi = 6.89 MPa).

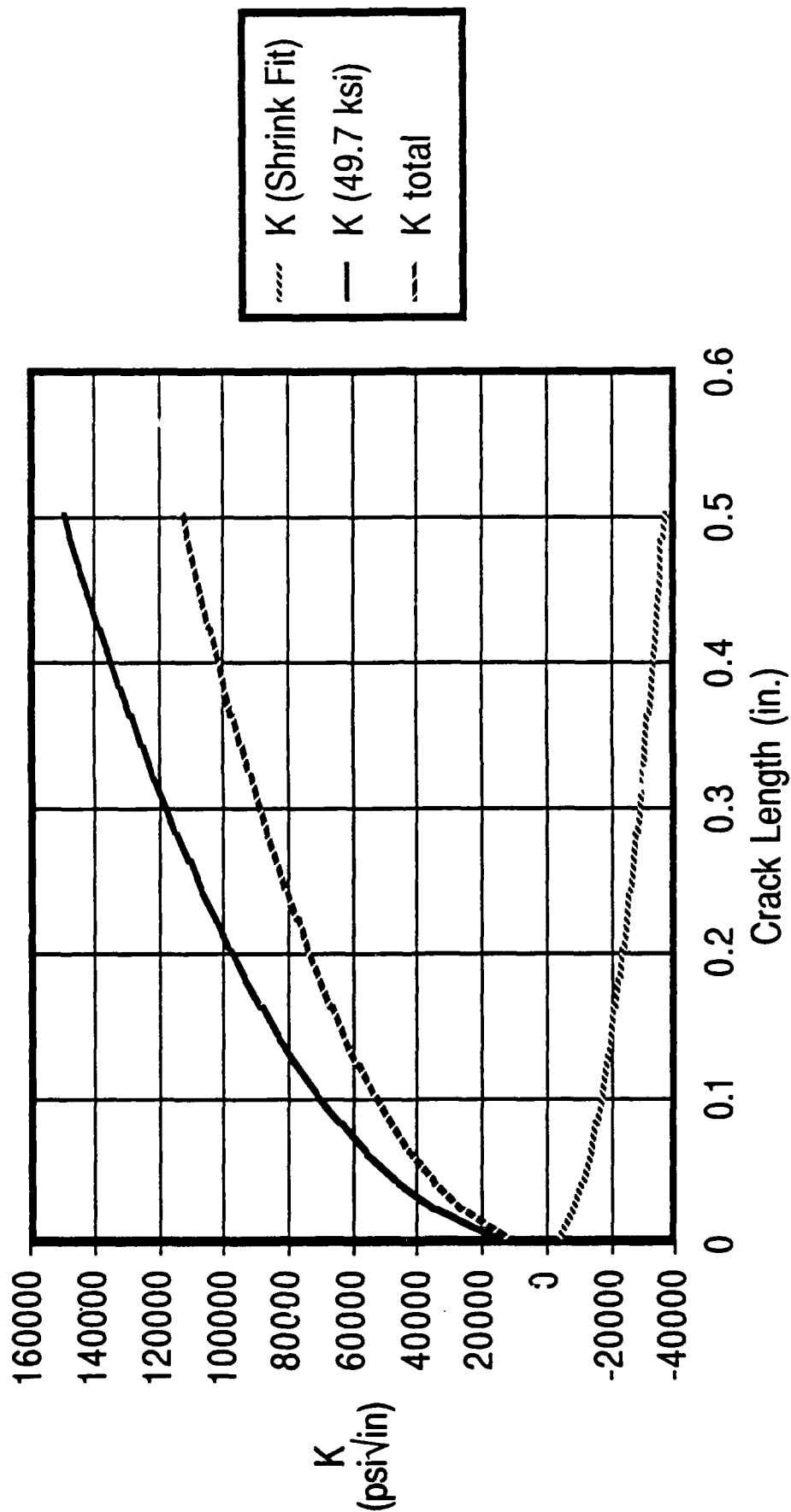


Figure 7. Specific K solution for 49.7 Ksi internal pressure
(1 Ksi = 6.89 MPa).

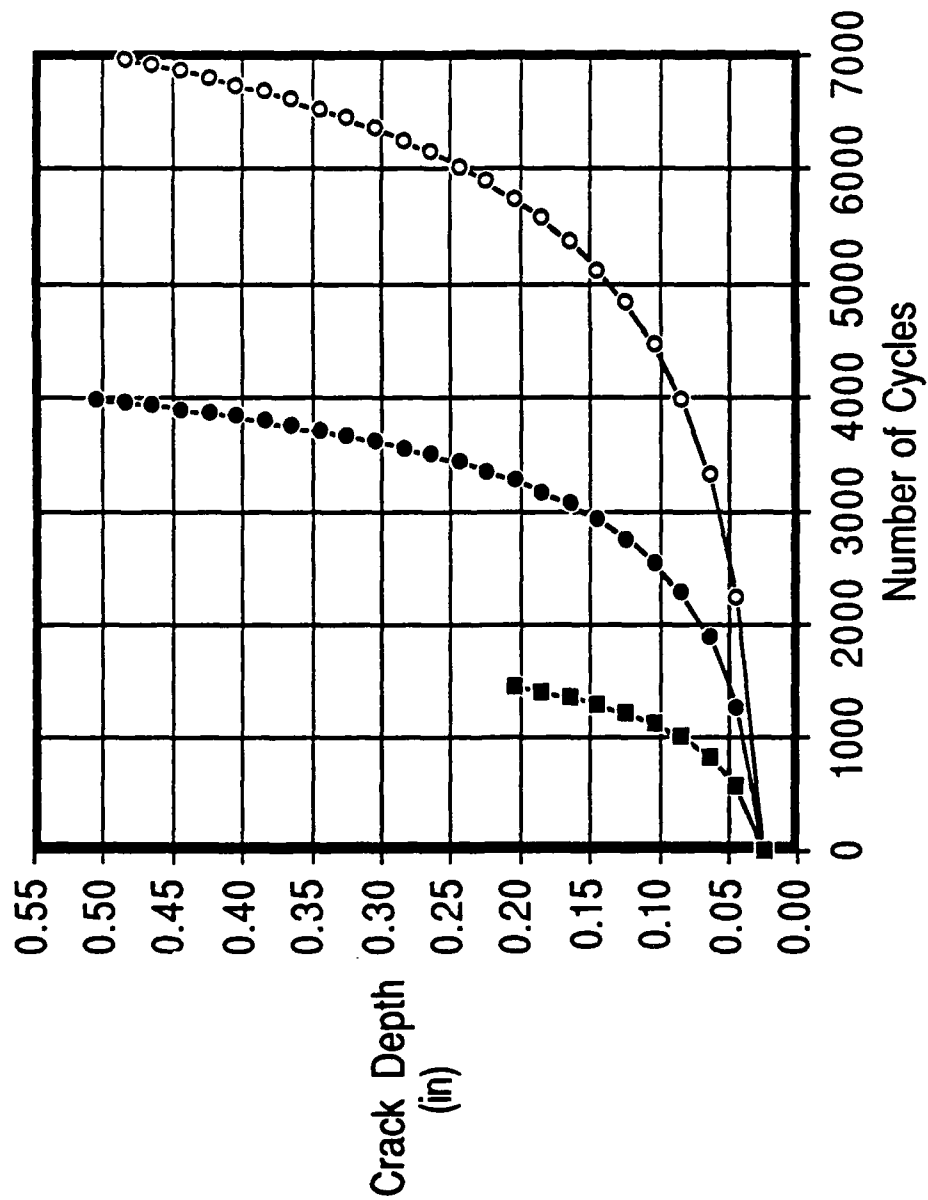


Figure 8. Remaining life predictions.

TECHNICAL REPORT INTERNAL DISTRIBUTION LIST

	<u>NO. OF COPIES</u>
CHIEF, DEVELOPMENT ENGINEERING DIVISION	
ATTN: SMCAR-CCB-D	1
-DA	1
-DC	1
-DM	1
-DP	1
-DR	1
-DS (SYSTEMS)	1
CHIEF, ENGINEERING SUPPORT DIVISION	
ATTN: SMCAR-CCB-S	1
-SE	1
CHIEF, RESEARCH DIVISION	
ATTN: SMCAR-CCB-R	2
-RA	1
-RM	1
-RP	1
-RT	1
TECHNICAL LIBRARY	5
ATTN: SMCAR-CCB-TL	
TECHNICAL PUBLICATIONS & EDITING SECTION	3
ATTN: SMCAR-CCB-TL	
DIRECTOR, OPERATIONS DIRECTORATE	1
ATTN: SMCWV-OD	
DIRECTOR, PROCUREMENT DIRECTORATE	1
ATTN: SMCWV-PP	
DIRECTOR, PRODUCT ASSURANCE DIRECTORATE	1
ATTN: SMCWV-QA	

NOTE: PLEASE NOTIFY DIRECTOR, BENET LABORATORIES, ATTN: SMCAR-CCB-TL, OF ANY ADDRESS CHANGES.

TECHNICAL REPORT EXTERNAL DISTRIBUTION LIST

	<u>NO. OF COPIES</u>		<u>NO. OF COPIES</u>
ASST SEC OF THE ARMY RESEARCH AND DEVELOPMENT ATTN: DEPT FOR SCI AND TECH THE PENTAGON WASHINGTON, D.C. 20310-0103	1	COMMANDER ROCK ISLAND ARSENAL ATTN: SMCRI-ENM ROCK ISLAND, IL 61299-5000	1
ADMINISTRATOR DEFENSE TECHNICAL INFO CENTER ATTN: DTIC-FDAC CAMERON STATION ALEXANDRIA, VA 22304-6145	12	DIRECTOR US ARMY INDUSTRIAL BASE ENGR ACTV ATTN: AMXIB-P ROCK ISLAND, IL 61299-7260	1
COMMANDER US ARMY ARDEC ATTN: SMCAR-AEE	1	COMMANDER US ARMY TANK-AUTMV R&D COMMAND ATTN: AMSTA-DDL (TECH LIB) WARREN, MI 48397-5000	1
SMCAR-AES, BLDG. 321	1	COMMANDER US MILITARY ACADEMY	1
SMCAR-AET-O, BLDG. 351N	1	ATTN: DEPARTMENT OF MECHANICS WEST POINT, NY 10996-1792	
SMCAR-CC	1		
SMCAR-CCP-A	1	US ARMY MISSILE COMMAND	
SMCAR-FSA	1	REDSTONE SCIENTIFIC INFO CTR	2
SMCAR-FSM-E	1	ATTN: DOCUMENTS SECT, BLDG. 4484	
SMCAR-FSS-D, BLDG. 94	1	REDSTONE ARSENAL, AL 35898-5241	
SMCAR-IMI-I (STINFO) BLDG. 59	2		
PICATINNY ARSENAL, NJ 07806-5000			
DIRECTOR US ARMY BALLISTIC RESEARCH LABORATORY ATTN: SLCBR-DD-T, BLDG. 305	1	COMMANDER US ARMY FGN SCIENCE AND TECH CTR ATTN: DRXST-SD	1
ABERDEEN PROVING GROUND, MD 21005-5066		220 7TH STREET, N.E. CHARLOTTESVILLE, VA 22901	
DIRECTOR US ARMY MATERIEL SYSTEMS ANALYSIS ACTV ATTN: AMXSU-MP	1	COMMANDER US ARMY LABCOM MATERIALS TECHNOLOGY LAB ATTN: SLCMT-IML (TECH LIB)	2
ABERDEEN PROVING GROUND, MD 21005-5071		WATERTOWN, MA 02172-0001	
COMMANDER HQ, AMCCOM ATTN: AMSMC-IMP-L	1		
ROCK ISLAND, IL 61299-6000			

NOTE: PLEASE NOTIFY COMMANDER, ARMAMENT RESEARCH, DEVELOPMENT, AND ENGINEERING CENTER, US ARMY AMCCOM, ATTN: BENET LABORATORIES, SMCAR-CCB-TL, WATERVLIET, NY 12189-4050, OF ANY ADDRESS CHANGES.

TECHNICAL REPORT EXTERNAL DISTRIBUTION LIST (CONT'D)

	<u>NO. OF COPIES</u>		<u>NO. OF COPIES</u>
COMMANDER US ARMY LABCOM, ISA ATTN: SLCIS-IM-TL 2800 POWDER MILL ROAD ADELPHI, MD 20783-1145	1	COMMANDER AIR FORCE ARMAMENT LABORATORY ATTN: AFATL/MN EGLIN AFB, FL 32542-5434	1
COMMANDER US ARMY RESEARCH OFFICE ATTN: CHIEF, IPO P.O. BOX 12211 RESEARCH TRIANGLE PARK, NC 27709-2211	1	COMMANDER AIR FORCE ARMAMENT LABORATORY ATTN: AFATL/MNF EGLIN AFB, FL 32542-5434	1
DIRECTOR US NAVAL RESEARCH LAB ATTN: MATERIALS SCI & TECH DIVISION CODE 26-27 (DOC LIB) WASHINGTON, D.C. 20375	1 1	METALS AND CERAMICS INFO CTR BATTELLE COLUMBUS DIVISION 505 KING AVENUE COLUMBUS, OH 43201-2693	1

NOTE: PLEASE NOTIFY COMMANDER, ARMAMENT RESEARCH, DEVELOPMENT, AND ENGINEERING CENTER, US ARMY AMCCOM, ATTN: BENET LABORATORIES, SMCAR-CCB-TL, WATERVLIET, NY 12189-4050, OF ANY ADDRESS CHANGES.